Molecular and Cellular Neuroscience 44 (2010) 154–164

Contents lists available at ScienceDirect

Molecular and Cellular Neuroscience

journal homepage: www.elsevier.com/locate/ymcne

ENA/VASP downregulation triggers cell death by impairing axonal maintenance in hippocampal neurons

D. Lorena Franco [a], Carolina Rezával [a], Alfredo Cáceres [b], Alejandro F. Schinder [c], M. Fernanda Ceriani [a,*]

[a] Laboratorio de Genética del Comportamiento, Fundación Instituto Leloir. Instituto de Investigaciones Bioquímicas-Buenos Aires (IIB-BA, CONICET), Argentina
[b] Laboratorio de Neurobiología y Biología Celular, Instituto Investigación Médica Mercedes y Martín Ferreyra-CONICET, 5016 Córdoba, Argentina
[c] Laboratorio de Plasticidad Neuronal, Fundación Instituto Leloir. Instituto de Investigaciones Bioquímicas-Buenos Aires (IIB-BA, CONICET), Argentina

ARTICLE INFO

Article history:
Received 1 July 2009
Revised 28 January 2010
Accepted 5 March 2010
Available online 15 March 2010

ABSTRACT

Neurodegenerative diseases encompass a broad variety of motor and cognitive disorders that are accompanied by death of specific neuronal populations or brain regions. Cellular and molecular mechanisms underlying these complex disorders remain largely unknown. In a previous work we searched for novel *Drosophila* genes relevant for neurodegeneration and singled out *enabled* (*ena*), which encodes a protein involved in cytoskeleton remodeling. To extend our understanding on the mechanisms of ENA-triggered degeneration we now investigated the effect of silencing *ena* ortholog genes in mouse hippocampal neurons. We found that ENA/VASP downregulation led to neurite retraction and concomitant neuronal cell death through an apoptotic pathway. Remarkably, this retraction initially affected the axonal structure, showing no effect on dendrites. Reduction in ENA/VASP levels blocked the neuritogenic effect of a specific RhoA kinase (ROCK) inhibitor, thus suggesting that these proteins could participate in the Rho-signaling pathway. Altogether these observations demonstrate that ENA/VASP proteins are implicated in the establishment and maintenance of the axonal structure and that a change on their expression levels triggers neuronal degeneration.

Introduction

Neuronal polarity is essential for input–output processing and appropriate flow of information in neuronal networks, contributing to the correct function of the nervous system (Sanchez-Soriano et al., 2007). The complex and polarized morphology of neurons is maintained and dynamically modified by microtubules and the actin cytoskeleton during brain development, which integrate external cues perceived through a number of signaling pathways giving rise to the appropriate morphological changes (Conde and Caceres, 2009). In this regard multiple studies have shown the importance of Rho-GTPases as well as its downstream target, the Rho A kinase (ROCK), in the regulation of actin dynamics during neuronal polarization (Bito et al., 2000; Da Silva et al., 2003). Once connectivity is established, it needs to be maintained throughout life to ensure integrity of the nervous system. However, the mechanisms involved in maintaining the structural integrity of the post mitotic brain remain poorly understood.

Among actin regulatory proteins, the ENA/VASP proteins are a conserved family which is critical for both filopodia formation and elongation. In vertebrates, this protein family is composed by Mena, VASP and EVL, whereas in *Drosophila enabled* (*ena*) is the only representative of this family (Gertler et al., 1996). All the members share a conserved domain structure that includes the N-terminal EVH1 domain (Ena/Vasp homology), the C-terminal EVH2 domain and a central proline-rich region. These proteins regulate the assembly of F-actin filaments by preventing the activity of capping proteins while supporting filament elongation (Applewhite et al., 2007; Lebrand et al., 2004). Given their function, it is expected that these proteins are localized in areas of dynamic actin remodeling, such as the external edge of the lamellipodia, the tips of the filopodia and the neuronal growth cones. Work carried out in *Drosophila*, *C. elegans* and mice showed that these proteins participate in axonal outgrowth, dendritic morphology, synapse formation and also function downstream of attractive and repulsive axon guidance pathways (Lanier et al., 1999; Li et al., 2005; Lin et al., 2007). Recent evidence shows that knocking out the three murine ENA/VASP proteins results in a blockade of axon fiber tract formation in the cortex *in vivo*, and that failure in neurite initiation is the underlying cause (Kwiatkowski et al., 2007; Dent et al., 2007). Interestingly, we have recently shown a new role for ENA in triggering progressive neurodegeneration in *Drosophila* (Rezával et al., 2008). In this previous work a functional mis-expression genetic screen was carried out to identify molecules involved in neurodegenerative processes,

* Corresponding author. Av. Patricias Argentinas 435, Buenos Aires (1405 BWE), Argentina. Fax: +54 11 5238 7501.
E-mail address: fceriani@leloir.org.ar (M.F. Ceriani).

1044-7431/$ – see front matter © 2010 Elsevier Inc. All rights reserved.
doi:10.1016/j.mcn.2010.03.004

and it was found that constantly reduced *ena* levels, as seen in the *ena*^{rev} mutant, triggers axonal transport defects and progressive degeneration in specific brain regions, likely through apoptosis.

Neurodegenerative diseases are characterized by a midlife onset and a progressive loss of a specific neuronal population. Age is a major risk factor for this group of disorders and the absence of effective therapies to prevent the onset, or delay the relentless progression underscores the need to improve our understanding of the molecular and cellular mechanisms underlying these pathologies (Bossy-Wetzel et al., 2004; Mattson and Magnus, 2006).

To increase our understanding on the mechanisms leading to neuronal degeneration we now investigated the effect of deregulation of *ena* ortholog genes in mouse hippocampal neurons. In order to inhibit the function of all family members, primary neuronal cultures were transfected with short interfering RNA pools (siRNAs). In agreement with our previous observations in flies, ENA/VASP down-regulation triggered apoptotic death in hippocampal neurons. Interestingly, neuronal death was preceded by the retraction of axonal projections. Finally, we identified a requirement for ENA/VASP function in concert with the RhoA signaling pathway for axonal growth and maintenance. Our results point to a central role of ENA/VASP in preserving neuronal polarity and survival.

Results

Efficient silencing of ENA/VASP family members employing small interfering RNAs

In *ena*^{rev} mutant flies, progressive neurodegeneration appears as a result of continuous silencing of the *enabled* gene (Rezával et al., 2008). To mimic such scenario and explore the molecular mechanisms underlying ENA/VASP-mediated neurodegeneration, the small interfering RNA (siRNA) technology was employed in cultured hippocampal neurons. An initial characterization showed that *ena*, *vasp* and *evl* mRNAs are expressed to a similar extent in cultured neurons maintained for up to 14 days in vitro (DIV), underscoring the need to target all of them in order to achieve an effective downregulation (Fig. 1A). For this purpose, we employed a specific siRNA pool for each member of this gene family (see Experimental methods); transfection efficiency was calculated employing a commercially available

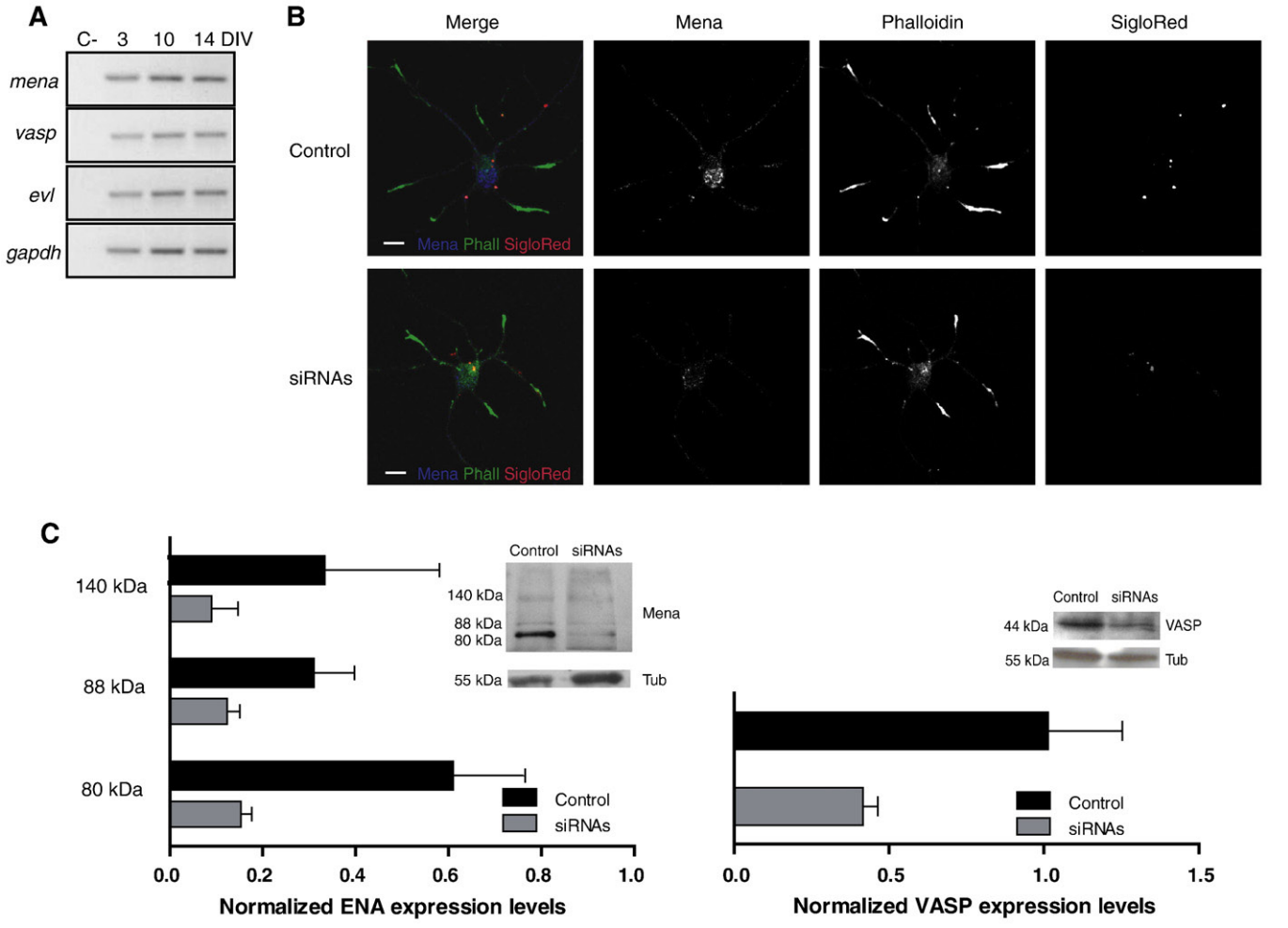

Fig. 1. Effective downregulation of the ENA/VASP family members in cultured hippocampal neurons from mouse embryos. (A) The expression of *mena*, *vasp* and *evl* was analyzed by semi-quantitative RT-PCR. Total RNA was prepared from cultured neurons at the indicated days in vitro (DIV). Expression of *gapdh* was measured as a normalization control. The C^- lane shows the result of amplification in the absence of template. (B) Representative immunofluorescence images of neurons transfected at 3 DIV with scrambled-siRNA pool and si-Glo Red, marker of transfection efficiency (control) or with a mixture of *mena*, *vasp* and *evl*-specific siRNA pools and si-Glo Red marker (siRNA). Cultures were fixed at 6 DIV and stained with a Mena specific antibody, as well as Phalloidin, to mark all F-actin processes. Note that Mena fluorescence was considerably decreased in neurons treated with the siRNA pools. Red fluorescent dots denote the uptake of the siRNA pools (efficiency control). Immunofluorescence was repeated >3 times with similar results. Scale bar: 10 μm. (C) Quantitative analysis of the levels of ENA or VASP proteins in neurons transfected at 3 DIV with a mixture of the three specific siRNA pools. Remaining protein levels were determined by Western blot analysis at 72 h post transfection (6 DIV). Normalized Mena/Tubulin (Tub, left panel) or VASP/Tub (right panel) ratios show a reduction of ~60–70% and ~60% for each isoform of Mena and VASP, respectively. All experiments (three in total) were carried out using si-RNAs at a concentration of 200 nM.

fluorescent RNA duplex (termed siRNA-Glo Red), and it averaged 40%. To examine the silencing efficiency of each siRNA pool, hippocampal neurons maintained for 3 DIV were transfected and the expression levels of each gene were analyzed 48–72 h post-transfection by immunofluorescence, Western blot and semi-quantitative RT-PCR. Under these conditions we found that expression of *mena*, *vasp* and *evl* was reduced by 40%, 60%, and 40% respectively (Supplementary Fig. 1A and B). Similar results were obtained after co-transfection of the three siRNA pools together along with the siRNA-Glo marker (Fig. 1B and C). Transfection and internalization of the siRNA was highly efficient as monitored by the localization and the intensity of the co-transfected fluorescent marker (Fig. 1B). The different Mena isoforms were reduced between 60% and 70%, meanwhile VASP levels were reduced by 60%, suggesting that the presence of the additional siRNAs did not result in a more efficient silencing of the other members of the family, underscoring their specificity. These results indicate that the expression of ENA/VASP family members in mouse hippocampal neurons is effectively reduced through this strategy.

Downregulation of ENA/VASP levels triggers apoptotic neuronal death

In ena^{rev} flies, continuous downregulation of *ena* levels throughout the lifespan is associated with an increase of programmed cell death in aged individuals (Rezával et al., 2008). On the other hand, the Mena/VASP/EVL triple knock-out mice did not show any sign of apoptosis (Kwiatkowski et al., 2007), although it displayed defects in ventricle size and total brain matter, which could derive from loss of neuronal tissue. Thus, to our knowledge, a correlation between ENA/VASP dysfunction and cell death has not been thoroughly explored in any mammalian system. To examine whether the acute reduction of the levels of ENA/VASP proteins could also trigger this phenomenon in cultured mammalian neurons, the highly specific TUNEL staining was performed (Fig. 2). Neurons (3 DIV) transfected with a scrambled-siRNA pool (control) displayed <10% TUNEL positive cells, assessed 48 h later. However, >30% neurons exhibited nuclear TUNEL signal when transfected with a mixture of the *ena*, *vasp* and *evl* siRNAs. These results show that an acute reduction in the ENA/VASP family levels induces cell death, at least in part through apoptotic mechanisms, underscoring its conservation between flies and mice.

Downregulation of ENA/VASP induces neurite retraction

To understand how downregulation of ENA/VASP could result in neuronal apoptosis we focused on previous knowledge on the canonical function of this gene family. ENA/VASP has been primarily implicated in the regulation of the dynamics of the actin cytoskeleton, which is critical in the generation of the initial processes giving rise to axon and dendrites (Dent et al., 2007; Kwiatkowski et al., 2007). We therefore monitored alterations in neuronal morphology in response to ENA/VASP dysfunction to investigate a possible link with apoptotic death. The maturation of hippocampal neurons in culture follows a well defined set of stages (Dotti et al., 1988). Upon plating, these cells form lamellipodia around the cell body (stage 1) that after 12–24 h condense to form three to four minor neurites (stage 2). From this pool of morphologically indistinguishable neurites one process starts to grow to become the axon (stage 3). The axon formation is a hallmark of neuronal polarization, as it marks the initial break in symmetry during neuronal development (Dotti and Poo, 2003). At 3–4 DIV minor processes develop into longer (over 40 μm) and branched dendrites, which taper in diameter as they extend distally (stage 4) (Bartlett and Banker, 1984). Thus, we evaluated the consequences of ENA/VASP downregulation on the morphology of polarized neurons, at the same stage in which apoptotic death was observed.

Three DIV neurons were transfected with control or siRNAs, fixed at 5 DIV and double-stained with FITC-phalloidin that labels F-actin (all neurites), and Tau-1 antibody that specifically labels axons. Representative images are included in Fig. 3A. Confocal images revealed a stage 4 morphology with a well-defined axon and several dendrites in the majority of control neurons (Fig. 3A, upper panel). In contrast, neurons treated with siRNAs were almost equally distributed among stages 2 and 4, and an abnormal "retracted" phenotype (Fig. 3A, bottom panel, arrowheads). Retracted neurons often exhibited two to three short neurites, or, in the most extreme examples, a single short process, usually staining positive for Tau-1. Evidence of distal axonal fragmentation could even be seen in neurons displaying less aberrant phenotypes (bottom panel, right).

A careful evaluation of neuron morphology by phase contrast microscopy along the course of several days revealed that the majority of control neurons remained in stage 4 throughout the experiment (up to 7 DIV). On the other hand, in siRNA treated cells, initially undistinguishable from control ones, we observed a striking reduction in the percentage of neurons in stage 4 starting 48 h after transfection, with a consequent increase in the retracted phenotype, which by the end of the experiment reached about 50% of siRNA-treated neurons (Fig. 3B). Forty-eight hours post transfection was selected for further analysis as the earliest timepoint displaying significant differences between control and siRNA-treated neuronal populations. Interestingly, individual downregulation of *ena*, *vasp* or *evl* did not result by itself in any morphological phenotype, supporting a functional redundancy among family members (data not shown and (Lanier et al., 1999; Menzies et al., 2004).

These data indicate that silencing *Mena*/*vasp*/*evl* induces neurite retraction in polarized neurons.

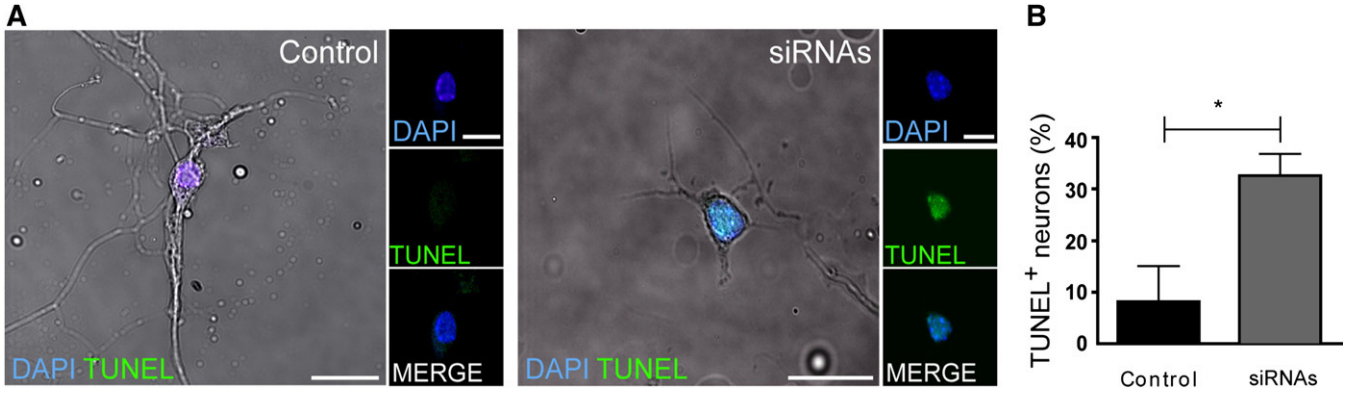

Fig. 2. ENA/VASP downregulation triggers apoptotic cell death. (A) Representative confocal images of TUNEL staining of neurons transfected at 3 DIV with scrambled-siRNA (control) or with a mix of Mena/Vasp/Evl siRNA pool (siRNAs) and fixed at 5 DIV. Scale bar: 20 μm. Insets on the right show magnified views of the nuclear area. Note the positive TUNEL signal in the nucleus of a siRNA transfected neuron, which is absent in the nucleus of the control. Scale bar: 10 μm. (B) Quantitative analysis of TUNEL staining showing an increase in the percentage of apoptotic cell death in treated neurons respect to controls (*$p<0.05$). About 80 to 100 neurons were counted per condition. Statistical analysis was done with Student's *t*-test.

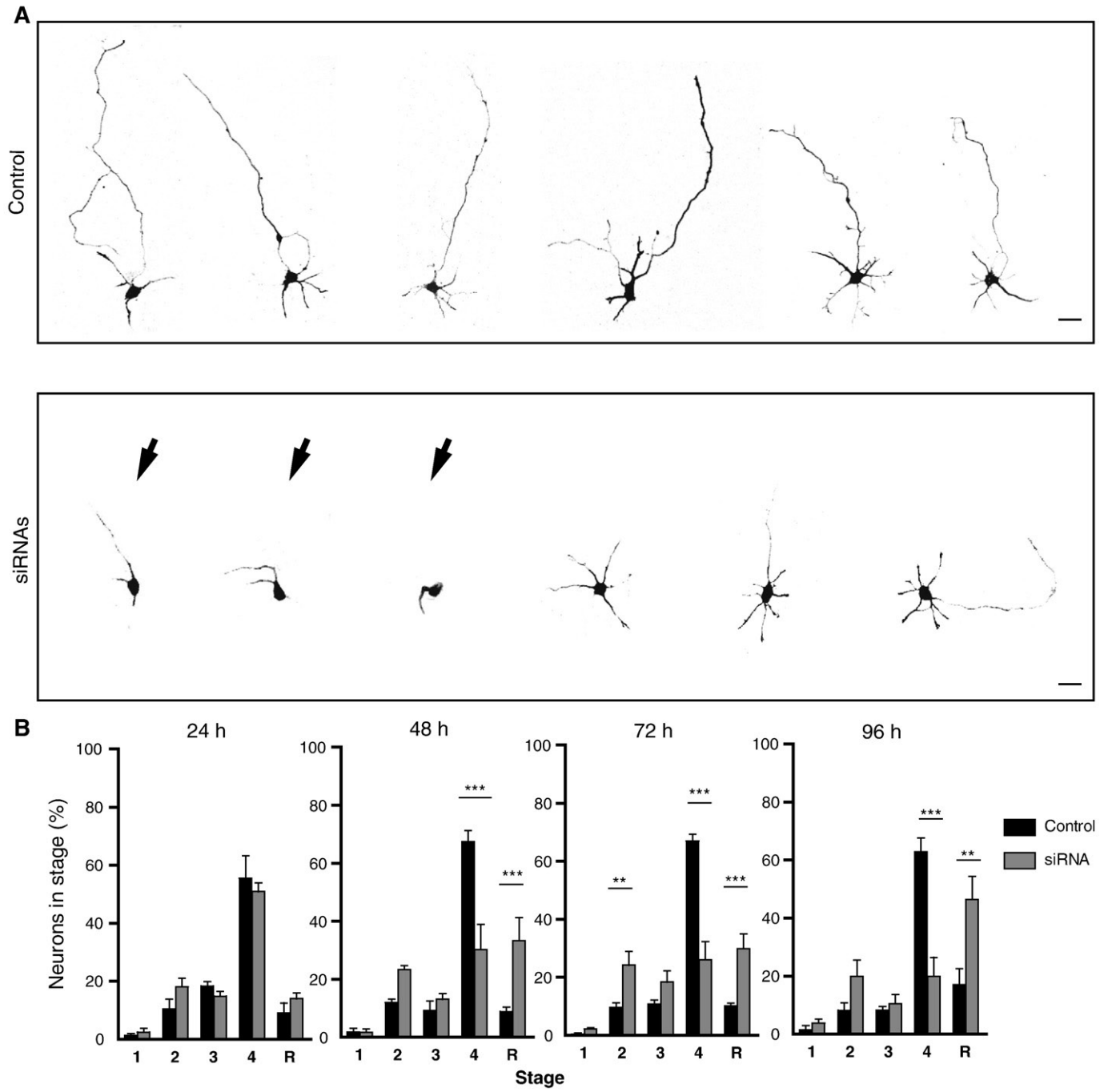

Fig. 3. Knock-down of the ENA/VASP family members induces neurite retraction. (A) Confocal images showing examples of neurons transfected at 3 DIV with control or siRNA pools (siRNAs), fixed at 5 DIV and stained with phalloidin-FITC and Tau-1 antibody. Merged images (inverted) show examples of the diversity of phenotypes observed for each treatment. Neurons displaying the retracted phenotype are indicated (arrowheads). Scale bar: 20 μm. (B) Neurons were transfected at 3 DIV and morphology was evaluated by DODT infrared contrast microscopy at each indicated time point. Staging was performed blind. Statistic analysis was performed by a two-way ANOVA followed by a Bonferroni posthoc test to compare control vs. siRNAs. $^{**}p<0.01$; $^{***}p<0.001$ ($n=5$ experiments).

Neurite retraction precedes apoptotic cell death

One interesting possibility to consider is that structural defects elicited by ENA/VASP downregulation give rise to neuronal death. Alternatively, axonal retraction might be a consequence of cell death (discussed in Luo and O'Leary, 2005). To determine whether neurite retraction in siRNA treated cells is cause or consequence of the apoptosis induced by downregulation of ENA/VASP, hippocampal cultures were treated with a general caspase inhibitor. If neurite retraction was a consequence of a cell death program the inhibitor should prevent this phenomenon. In contrast, if neurite retraction preceded cell death, caspase blockade should have no impact on the morphological changes induced by downregulation of ENA/VASP levels.

Addition of the Ac-DEVD-CHO caspase inhibitor right after transfection effectively prevented apoptosis. A similar percentage of control and siRNA treated neurons survived in the presence of the inhibitor (Fig. 4A). Strikingly, siRNA transfected neurons displayed a similar array of phenotypes regardless of whether the inhibitor was included (Fig. 4B). Under both conditions, a reduction of stage 4 neurons together with an increase in the retracted phenotype was observed, and no significant differences were found between siRNA treated groups.

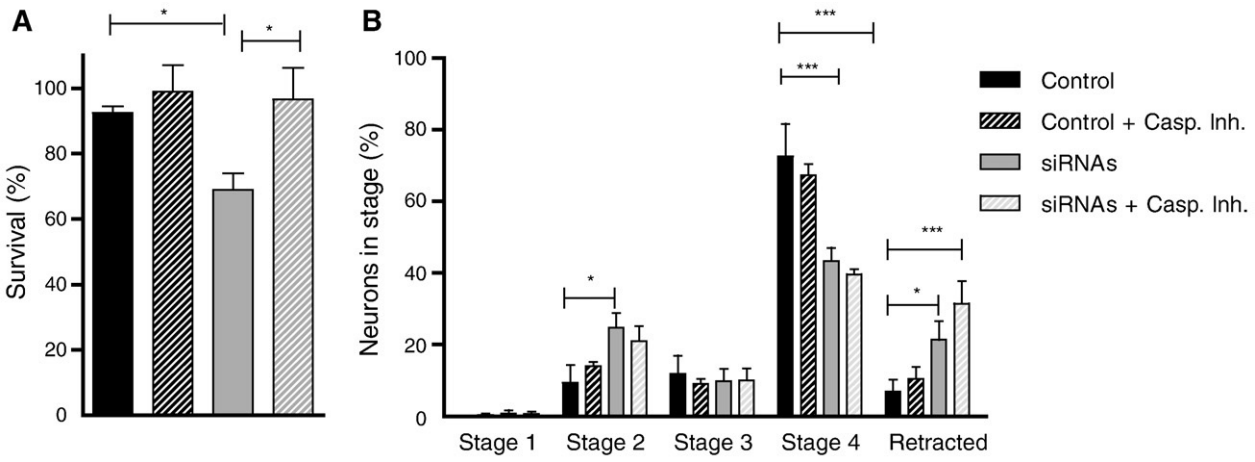

Fig. 4. Neurite retraction precedes apoptosis. (A) Addition of siRNAs in 3 DIV neurons reduced survival as assessed 48 h later. Addition of a specific caspase inhibitor (Ac-DEVD-CHO, 50 μM) rescued cell death. Statistical analysis included a one-way ANOVA followed by a Tukey's multiple comparison test with $^{*}p<0.05$ ($n=5$ experiments). (B) Neurite retraction precedes cell death. Three DIV neurons were transfected as in A, and caspase inhibitor (50 μM) was added right after transfection. The percentage of neurons in each stage was determined 48 h post-transfection (5 DIV). Staging was performed blind. Statistic analysis was done using a two-way ANOVA followed by a Bonferroni posthoc test for control vs. siRNAs ($^{*}p<0.05$; $^{***}p<0.001$) and control vs. siRNA + Inh ($^{***}p<0.001$); $n=3$ experiments.

These data demonstrate that downregulation of ENA/VASP induces neurite retraction and subsequent apoptotic death.

ENA/VASP family is required for axonal specification and maintenance of the axonal structure

To characterize in more depth the structural changes that resulted from the continuous impaired function of the ENA/VASP protein family, 3 DIV control and siRNA transfected neurons were immunostained using the axonal marker Tau-1 and FITC-phalloidin. Representative images are included (Fig. 5A). Analysis of the neuronal morphology revealed that the number of axons, defined as Tau-1 positive processes longer than 60 μm, was affected. While >80% of control neurons displayed a single axon and even an additional 10% displayed two, ~40% of siRNA-treated cells exhibited no axons, and roughly 60% displayed just one, suggesting that ENA/VASP downregulation impinges upon this structure (Fig. 5B, left panel). Among the siRNA-treated population still containing an axon there was a significant decrease in axonal length compared to controls, suggesting that preexisting axons can undergo retraction by ENA/VASP dysfunction (Fig. 5B, right panel).

To determine if this retraction specifically affected the axonal structure, the number and length of the Tau-1 positive and negative processes were also analyzed (Fig. 6B). The overall length of Tau-1 positive processes was considerably reduced in treated neurons, whereas the number did not change significantly. In contrast, neither the number nor the length of Tau-1 negative processes changed significantly between control and siRNA transfected neurons. These data show that a reduction of ENA/VASP levels specifically affects the maintenance of the axonal structure sparing dendrites.

The role of the ENA/VASP family has been extensively characterized during development (Drees and Gertler, 2008). Moreover, recent studies have shown that ENA/VASP/EVL deficient cortical neurons fail to elaborate filopodia, and thus they are unable to extend processes (Dent et al., 2007). To further examine whether downregulation of ENA/VASP levels could specifically inhibit axonal outgrowth during neuritogenesis, neurons were transfected at stage 1 (before plating) with control or mixed siRNAs, and their ability to develop an axon was analyzed. When 0 DIV neurons were examined, two thirds of control neurons exhibited a single axon, while the remaining had none. The opposite scenario was observed in siRNA treated cells, where the majority of neurons did not form axons (Fig. 5C and D). Under these conditions a proportion of the si-RNA treated neurons developed one or two processes reminiscent of those seen in the control population (Fig. 5D), likely pointing to the fraction of untransfected neurons.

Taken together, our observations demonstrate that ENA/VASP proteins are critical for the establishment and maintenance of neuronal polarity. Reduced expression of ENA/VASP induces axonal retraction and the onset of neuronal death.

ENA/VASP interacts with the RhoA/ROCK signaling pathway

It is well established that small GTPases, such as RhoA and its downstream target Rho-associated kinase (ROCK), are involved in the regulation of neuritogenesis (Bito et al., 2000) as well as in neurite retraction (Katoh et al., 1998). On the other hand, ENA/VASP proteins link signaling pathways to the remodeling of actin cytoskeleton in neuritogenesis (Drees and Gertler, 2008) and in axonal retraction (Fig. 5), suggesting a potential connection between both protein families. A potential role of the RhoA/ROCK signaling pathway in the maintenance of axonal structure was evaluated using a specific inhibitor of this protein, Y-27632 (Ishizaki et al., 2000). Polarized neurons (3 DIV) were transfected with siRNA pools and incubated with Y-27632. After 2 days neurons were fixed and stained with FITC-phalloidin and anti Tau-1 antibody and a detailed characterization of all neurite processes was performed (Fig. 6). Addition of ROCK inhibitor increases the number of neurites on polarized (3 DIV) neurons as it has been shown for undifferentiated (0 DIV) neurons (Da Silva et al., 2003). In fact, we observed a specific increase in the number of Tau-1 positive processes, rendering the Tau-1 negative ones unaffected, in agreement with a recent report (Sanchez et al., 2008). Neurite length was not affected in either case (Fig. 6B, bottom panel). Intriguingly, a reduction in ENA/VASP levels prevented the increase in the number of processes induced by Y-27632; thus, transfected neurons in the presence of the ROCK inhibitor displayed the typical neuronal morphology that follows ENA downregulation, suggesting that silencing this family obliterated the effect of the inhibitor. In agreement with these observations, the addition of this ROCK inhibitor did not rescue the neuritogenesis defect in cultured neurons obtained from the ENA/VASP/EVL triple KO mice (Dent et al., 2007). Altogether these data suggest that ENA/VASP proteins could participate in the Rho-signaling pathway, potentially downstream of ROCK in the maintenance of the axonal structure.

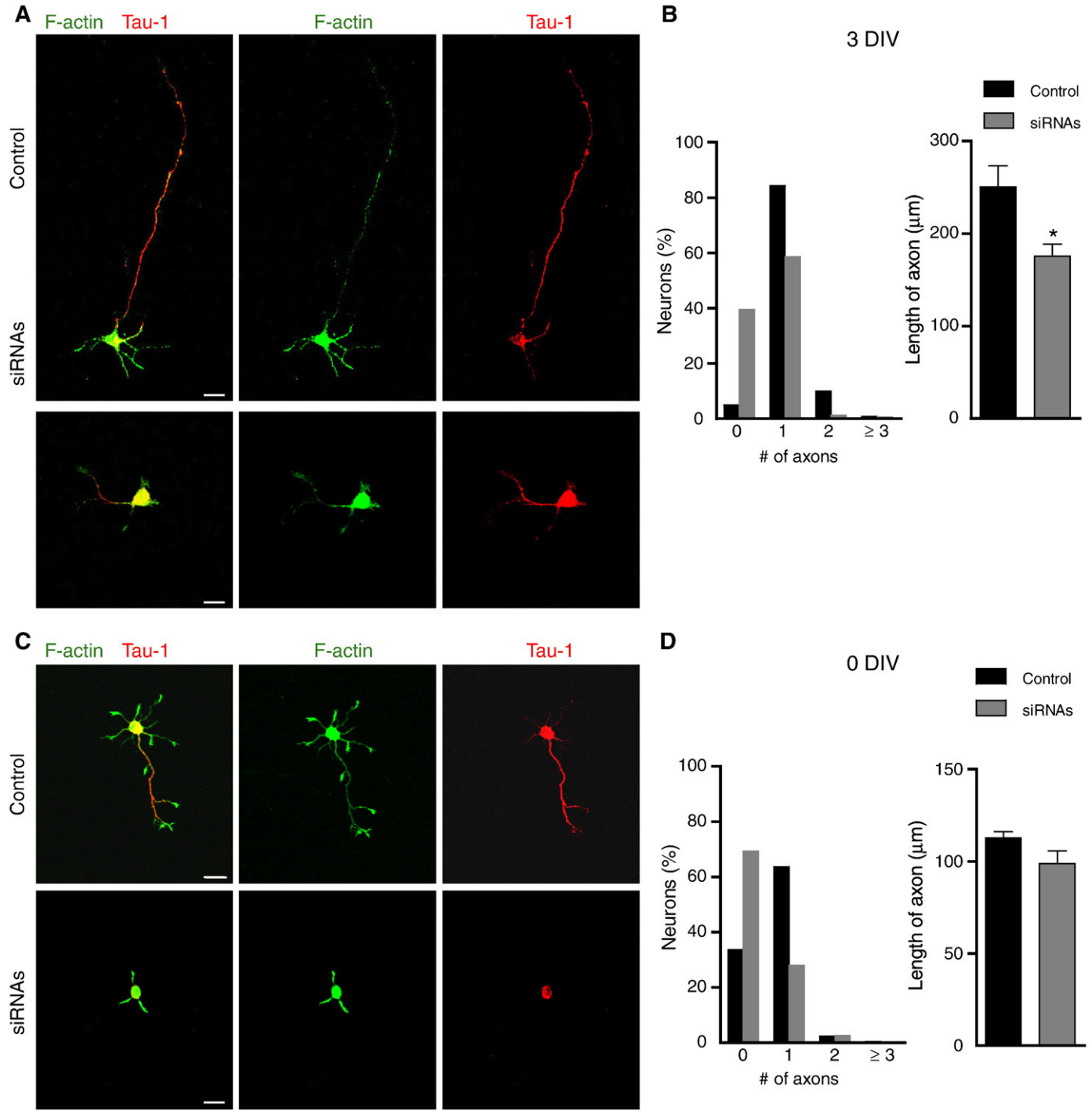

Fig. 5. ENA/VASP deregulation specifically affects axon maintenance (A, B) and interferes with the establishment of neuronal polarity (C, D). (A) Representative confocal images of neurons transfected at 3 DIV with control or siRNA pools, fixed at 5 DIV and stained with FITC-phalloidin and anti Tau-1 antibody. Scale bars: 20 µm. (B) Left panel: Relative frequency histogram displaying the number of axons per neuron, (defined as a Tau^+ process with >60 µm in length). Right panel: Axonal length in neurons displaying one axon or more. Quantitation was performed blind. Statistical analysis was done by Student's *t*-test ($^*p<0.05$, $n=4$ experiments). (C) Representative confocal images of neurons transfected before plating (0 DIV) with control or siRNAs, and fixed and stained 72 h later. Scale bars: 20 µm. (D) Relative frequency histogram displaying the number of axons per neuron (left panel) and axonal length (right panel). No significant differences were observed ($n=5$ experiments).

Discussion

Neurodegeneration is a process by which neurons lose their structure and function as a result of a pathological condition (Palop et al., 2006). This phenomenon affects a broad range of organisms from invertebrates to human (Lessing and Bonini, 2009). The observed similarities in all neurodegenerative diseases suggest that these disorders share common characteristics in their pathogenesis and, hence, some molecular and cellular mechanisms might be conserved among them. We have developed a functional mis-expression genetic screen in *Drosophila* to identify molecules involved in progressive degeneration. One of the isolated mutants displaying constantly reduced *ena* levels develops in time axonal transport defects and progressive degeneration likely through apoptosis (Rezával et al., 2008). In this work we show that the deregulation of ENA/VASP family in hippocampal neurons leads to axonal retraction followed by apoptotic neuronal death, suggesting that

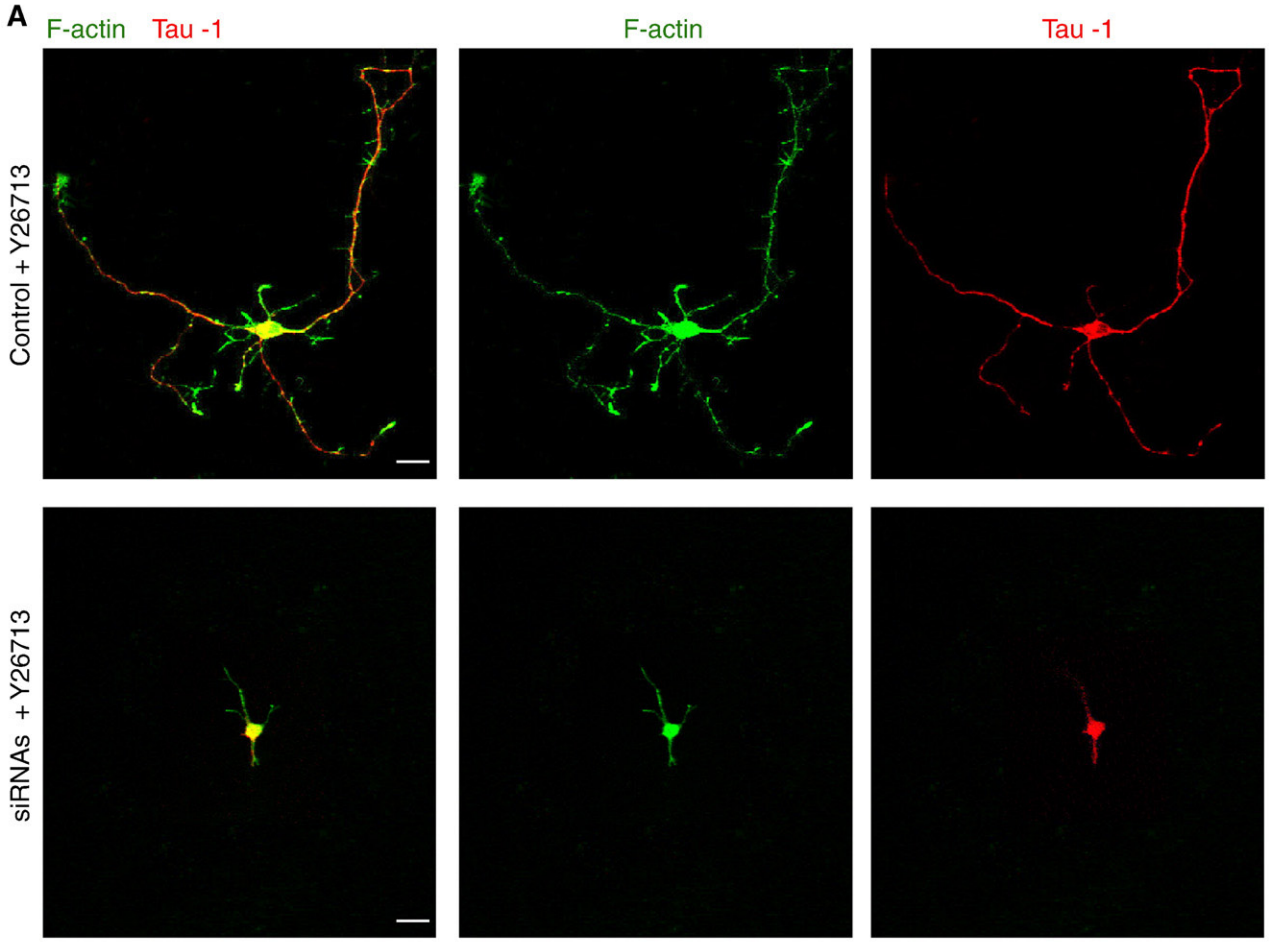
A
F-actin Tau -1
F-actin
Tau -1
Control + Y26713
siRNAs + Y26713

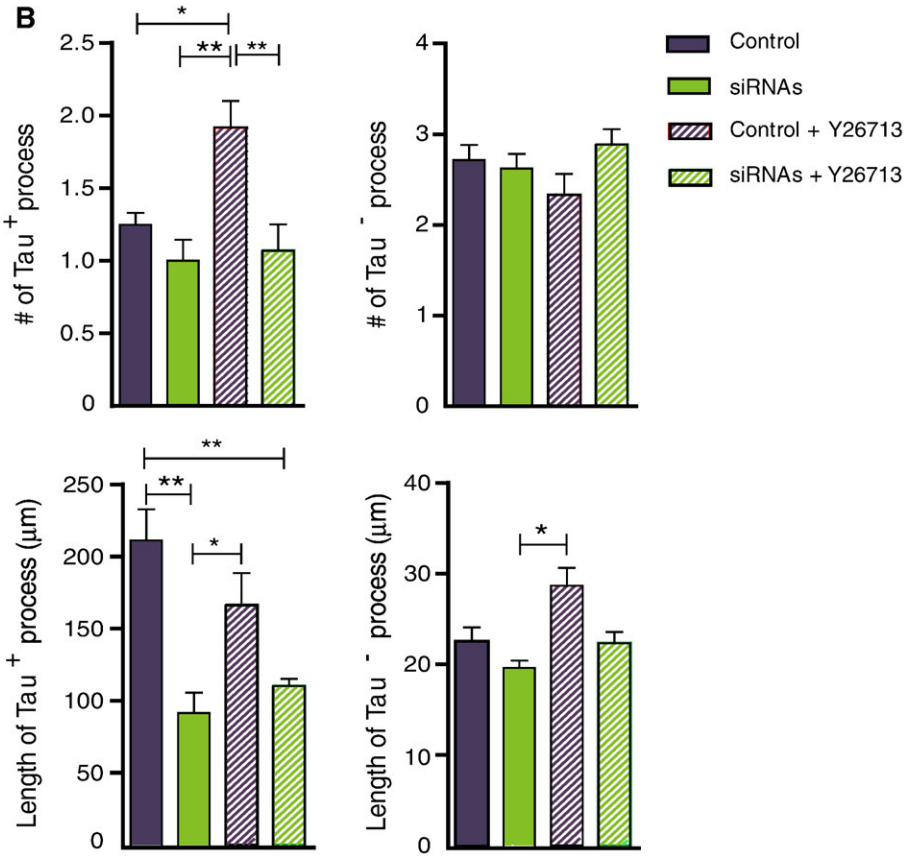
B
Control
siRNAs
Control + Y26713
siRNAs + Y26713
# of Tau+ process
# of Tau- process
Length of Tau+ process (µm)
Length of Tau- process (µm)

the mechanisms of ENA/VASP-mediated neurodegeneration are conserved in flies and mice.

Understanding how ENA/VASP depletion leads to axonal retraction

The role of the ENA/VASP family members on the regulation of actin-cytoskeleton dynamics has been intensively studied in the last decade (Drees and Gertler, 2008). Nevertheless, previous work focused on the role of this family during development of the nervous system by chronic knockout or by forced delocalization of the ENA/VASP proteins (Lanier et al., 1999; Bear et al., 2002; Kwiatkowski et al., 2007).

In this study we demonstrated that reduced ENA/VASP levels lead to neuronal degeneration through axonal retraction in polarized neurons. This finding indicates that ENA/VASP proteins are required not only during filament elongation but also for the maintenance of axonal integrity, and thus the absence of this protein family would result in a collapse of the structure. It has been shown that inhibition of F-actin turnover results in axonal retraction, which would provide a simplistic explanation to our results (Gallo et al., 2002). However, direct cytoskeletal disassembly does not necessarily lead to cell death as it has been shown in rat cerebral ganglion neurons (Linseman et al., 2001), thus suggesting a more complex scenario where ENA/VASP depletion would affect additional components (see below).

Given that this family is localized in dendrites as much as in axons (Giesemann et al., 2003; Lin et al., 2007) it is surprising that ENA/VASP downregulation initially triggered axonal degeneration without affecting dendrites (Figs. 3B and 6B). This might reflect a higher vulnerability of the axonal compartment to silencing the ENA/VASP family. Minor processes would eventually be affected, either directly or as a consequence of axonal retraction. While the basis of such specificity is yet to be investigated several scenarios can be considered. It has been shown that acetylated, more stable, microtubules are a landmark of axonal identity (Gomis-Ruth et al., 2008). Since the existence of a cross-talk between the actin cytoskeleton and the microtubule network has also been demonstrated (Myers et al., 2006; Bradke and Dotti, 2000), it would be possible to speculate that ENA/VASP could somehow modulate the stability of microtubules, thereby affecting not only axonal identity but also its maintenance. The fact that loss of ENA/VASP function inhibits neuritogenesis in undifferentiated neurons could result from an altered interaction between the actin and microtubule systems (Dent et al., 2007). Rho GTPases are critical regulators of the actin cytoskeleton in eukaryotic cells. In particular, these proteins control neurite outgrowth and retraction (Jalink et al., 1994; Luo et al., 1994; Arimura and Kaibuchi, 2007). The serine threonine Rho-associated kinase (ROCK) is an important mediator of RhoA activity in neurite retraction, as inhibiting this kinase activity completely reverted RhoA-mediated retraction in cultured hippocampal pyramidal neurons (Nakayama et al., 2000). Many substrates have been identified for ROCK, but the most important in the context of axon retraction is the regulation of myosin regulatory light chain phosphorylation (Luo, 2002). Silencing ENA/VASP interfered with the RhoA signaling pathway (Fig. 6). Since ENA/VASP are substrates of a number of different kinases such as ABELSON (Comer et al., 1998), Protein Kinase A (Lebrand et al., 2004) and Protein Kinase G (Butt et al., 1994), it is tempting to speculate that ENA/VASP could be a direct target of ROCK in controling the maintenance of axonal structure. However, alternative scenarios are also possible. The fact that the addition of ROCK inhibitor could not rescue the ENA/VASP triggered defect could also imply that both protein groups are involved in parallel pathways. Under these conditions depleting ENA/VASP levels would not necessarily impact the state of the RhoA signaling. To explore this possibility we measured the levels of activated RhoA after transfection with controls and the mixture of si-RNA pools. No significant differences were observed (Supplementary Fig. 2), underscoring that axonal retraction induced by ENA/VASP does not imply activation of the RhoA signaling pathway. Additional experiments would be required to unequivocally establish whether Mena/VASP are indeed downstream of this signaling cascade, and how this family interacts with other small GTPases (Higashi et al., 2009) that could also impinge upon the state of RhoA signaling.

ENA/VASP downregulation triggers apoptotic cell death

Previous reports on the consequences of the complete loss of ENA/VASP function did not find any indication of neuronal death (Kwiatkowski et al., 2007), in contrast to the results obtained in the RNAi-based hypomorph models in flies (Rezával et al., 2008) and mice (Fig. 2). Although the cause of this apparent discrepancy remains to be explored, the inherent nature of the models employed (the knock-out versus the RNAi-based technology) could at least partially account for the differences observed. One potential explanation is the different developmental timing in which the loss of this protein family becomes noticeable. In the knock-out mice or cultures derived from them, the complete absence of ENA/VASP could trigger some compensatory mechanism including the expression of different sets of genes which could instruct axon formation by an actin-remodeling cascade unrelated to ENA/VASP. Additionally, the RNAi technology is not 100% efficient, and acutely reduced levels of a wild type protein might alter the balance of interactions that usually control actin dynamics. Besides, in the RNAi-based model system only a proportion of cells are targeted for disruption in an otherwise normal tissue.

Several lines of evidence support the notion that deregulation of cell death programs are involved in neurodegenerative disorders such as Alzheimer's disease and Huntington's disease (Ona et al., 1999; Galvan et al., 2006; Graham et al., 2006; Bredesen et al., 2006). But, why does the reduction of ENA/VASP levels trigger apoptosis? Although the mechanism is not fully understood yet, some recent data could shed light on this issue. It has been demonstrated that ENA interacts with FE65, an adaptor protein that can also form a complex with the amyloid precursor protein (APP), which is relevant in the pathogenesis of Alzheimer's disease (Ermekova et al., 1997; Sabo et al., 2001). Moreover, recent evidence shows that FE65 can function as a core adaptor molecule in a multi-subunit transcriptional repressor, which can silence the expression of a caspase gene (*CASP4*) (Kajiwara et al., 2009). It is therefore tempting to speculate that the complex FE65-APP-ENA not only could play specific roles within the cytoplasm (Sabo et al., 2001; Ikin et al., 2007), but also act directly in the nucleus regulating gene expression. Thus, the FE65-APP-ENA complex could translate modifications in the state of the actin cytoskeleton to transcriptional regulation of genes relevant for cell survival (Zambrano et al., 1998; Cao and Sudhof, 2001; Kajiwara et al., 2009). From these findings emerges the possibility that ENA/VASP might directly or indirectly participate in the pathogenesis of Alzheimer.

Our findings provide experimental evidence that ENA/VASP proteins have a crucial participation in maintenance of the axonal structure and that a decrease in their expression levels could trigger axonal retraction, in turn inducing apoptosis. These results are in line with the evidence suggesting that some dysfunctions in actin-

Fig. 6. The Mena/VASP family participates in the RhoA-ROCK signaling pathway. (A) Three DIV neurons were transfected with control or the siRNA pools. ROCK inhibitor (Y-27632, 5–10 μM) was added as indicated immediately after transfection. Neurons were fixed at 5 DIV and stained with an antibody against Tau-1 and FITC-phalloidin. Scale bars: 20 μm. (B) Inhibition of the ROCK signaling cascade only affects the number and length of Tau $^{+}$ processes. A quantitative analysis of the number (upper panels) and length (bottom panels) of Tau^{+} and Tau^{-} processes was performed. Quantitation was performed blind. Statistic analysis was carried out by one-way ANOVA followed by a Tukey posthoc test with $n=4$ experiments.

cytoskeleton components, which are crucial for synapse formation and plasticity, could contribute to neurodegenerative diseases (McMurray, 2000).

Experimental methods

Neuronal cultures

Primary cultures of hippocampal neurons from embryonic mouse brain were prepared as described previously (Caceres et al., 1986). Briefly, hippocampi dissected from mouse embryos (embryonic day 18) were treated with trypsine (Invitrogen). Cells were dissociated by repeated pipetting and plated onto glass coverslips (12 mm in diameter) or onto dishes (60 mm in diameter) pre-treated with 0.5–1 mg/ml poly-L-lysine (Sigma-Aldrich Chemicals) at densities ranging from 300,000 (for immunocytochemistry) to 600,000 (for RNA and Western blot analysis). Cultures were maintained with DMEM plus 10% fetal bovine serum for 3 h, when the medium was replaced with Neurobasal media (Gibco) supplemented with B27 (Invitrogen). All cultures were maintained in a humidified 37 °C incubator with 5% CO_2.

Transient transfections with siRNA

Hippocampal neurons were transfected with 200 nM of each SMART pool small interfering RNA (Dharmacon) designed to silence mouse Mena, EVL, and VASP or with the control ON-TARGET plus Non-targeting Pool (Dharmacon). Each specific pool contained four doubled-stranded RNAs targeted to the following sequences. For mena: *mena:* 5′-AGCACUAAUUUGCGAUGUA-3′; *mena2:* 5′-GGGUAGUGGCUUAAUGGAA-3′; *mena3:* 5′-CAGCAGAGUACAUAUAUAU-3′; *Mena4:* 5′-CAUCAUAUGCUAAAGUCAU-3′. For EVL: *evl1:* 5′-AGAAGUGGGUACCGAUCAA-3′; *evl2:* 5′-CCGUCAGGUCUAUGGCUUA-3′; *evl3:* 5′-GGAGCAACUCGGUGGAGAA-3′; *evl4:* 5′-ACCAGCAGGUUGUGAUCAA-3′. For VASP: *vasp1:* 5′-UGCCAUUGCUGGAGCCAAA-3′; *vasp2:* 5′-AGGAAAUCAUCGAAGUCUU-3′; *vasp3:* 5′-GGGCUACUGUGAUGCUUUA-3′; *vasp4:* 5′-GAGCUGAGGAAGCGGGGUU-3′. Neurons of 3 days in vitro (3 DIV, stage 3) or neurons before plating (stage 1) were used for the experiments. Transient transfections were performed with Lipofectamine 2000 (Invitrogen) following the manufacturer's instructions. siGLO Red (Dharmacon) was used to monitor the efficiency of each transfection. Cells were harvested 72 h post-transfection and Mena levels were examined by inmunocytochemistry. Mena and VASP levels were also analyzed by Western blot 72 h post-transfection. In parallel *evl* levels were examined by semi-quantitative RT-PCR 48 h post-transfection since no commercial antibody is available. In experiments involving the ROCK inhibitor, 5–10 μM of Y-27632 (Calbiochem) was added whenever the transfection media was replaced; neurons were analyzed 48 h post-transfection. In experiments involving the caspase inhibitor, 50 μM of Ac-DEVD-CHO (Promega) was added whenever the transfection media was replaced and neurons were analyzed 48 h post-transfection.

A solution containing acridine orange and ethidium bromide was used to quantify the percentage of survival. Non-fixed cells were stained for 5 min in 500 μl of media containing 1 mg/l of acridine orange (labeling live neurons in green) and 20 mg/l of ethidium bromide (labeling dead neurons in red) (Trulzsch et al., 2007). Cells were rinsed with PBS and evaluated immediately by fluorescence microscopy. The survival rate in each condition was expressed as the percentage of the total number of cells. About 100 neurons derived from five independent cultures were analyzed per condition.

Semi-quantitative RT-PCR

Expression levels of the *Mena*, *vasp* and *evl* in cultured neurons or after RNA interference (siRNA) treatment were examined. Total RNA was isolated using Trizol (Invitrogen). Reverse transcription was performed employing the SuperScript first-strand synthesis system (Invitrogen) according to instructions of the manufacturer. Semi-quantitative PCR analysis was performed using the following primers: *menaFw* 5′-GCTCCCTGTCTAGTGCTCCA-3′; *menaRv* 5′-GGTGTAGGGGGTGTGGAAGT-3′; *vaspFw* 5′-CCACAACCCCACTGCTAACT-3′; *vaspRv* 5′-ACTGTATGGCGTCCTCCTTG-3′; *evlFw* 5′-GGCCTCATGGAAGAAATGAA-3′; *evlRv* 5′-GTTTCTCCACCGAGTTGCTC-3′. The products obtained at different cycles (26, 28, 30) were analyzed on agarose gels stained with ethidium bromide. Quantification was performed on products obtained in cycle 28 employing the Image J software. For quantification, *evl* expression levels were normalized to those of *gapdh*. Three independent experiments were carried out.

Western blot

To quantitate the efficiency of siRNAi-triggered downregulation, 3 DIV neurons were transfected with 200 nM of Mena and Vasp siRNA or the control pools. Three days post-transfection cells were harvested in RIPA buffer (deoxycholate, 0.5%; SDS 0.1%; NP40 1%; and EDTA, 5 mM in PBS 1× with a cocktail of general protease inhibitors (Sigma)) and incubated on ice for 20 min. Samples for electrophoresis were resuspended in loading buffer heated to 100 °C for 5 min and resolved by SDS-PAGE using 8–10% acrylamide. For Western blot equal amounts of samples were loaded. Proteins were transferred to a PVDF membrane for 2 h at 100 V, blocked with 5% BSA or 5% milk for 1 h at RT. Membranes were then incubated with rabbit anti-VASP antibody (1:2000; Calbiochem) or with mouse anti-ENA antibody (1:400; BD Transduction laboratory) in blocking solutions for 1 h up to over night at 4 °C before detection with HRP-conjugated secondary antibodies (1:2500; Jackson ImmunoResearch). Chemoluminescence was detected with ECL+ (Amersham Bioscience). Quantification of the bands was performed using Image J software. The expression levels of each isoform of Mena and VASP proteins were normalized to endogenous tubulin.

Immunofluorescence

Neurons were fixed at 4, 5, or 6 DIV (as indicated) with 4% paraformaldehyde in 4% sucrose-containing PBS and permeabilized in 0.2% Triton X-100 in PBS for 5 min. Then, neurons were blocked in 5% BSA in PBS for 1 h at room temperature (RT). Neurons were then incubated with anti Tau-1 antibody (1:800, a generous gift from L. Binder) for 1 h at RT. The secondary antibody used was Cy5-anti mouse antibody (1/250, Jackson ImmunoResearch) and co-incubated with FITC-phalloidin (Sigma Chemicals) for 1 h at RT. After staining, neurons were washed with PBS, mounted, and visualized with a Zeiss 510 Meta confocal microscope. To analyze Tau^+ and Tau^- processes, co-stained cells were randomly selected; the number and length of each process was determined employing the LSM Image Browser software. A total of 150 neurons derived from four independent cultures were analyzed blind for each condition.

For a direct comparison of Mena levels between control and siRNA transfected neurons confocal fluorescence images were taken employing the same settings. TUNEL staining was performed according to the manufacturer's recommendations (Apoptag Plus Fluorescein *in situ* apoptosis detection Kit, Chemicon International S7111). Co-localization with DAPI was used as counter-stain.

Morphological analysis

To determine the proportion of neurons in each stage of development (Figs. 3B and 4B) 10 representative pictures of random fields from control and siRNAs transfected neurons were taken using a Zeiss Axiovert 135 M inverted microscope with a 10× phase contrast objective. Images were captured with a CCD camera (Hamamatsu Digital Camera C4742-95). One hundred neurons were analyzed blind for each condition.

Rho activity assays

The enzyme-linked immunosorbent assay (ELISA)-based G-LISA kit (Cytoskeleton, Denver, CO; catalogue number BK124) was used to determine endogenously active RhoA levels in neurons according to the manufacturer's instructions. In brief, neurons transfected with control pools or with the mixture of the three si-RNA pools were lysed 48 h post transfection in 50 µl of G-LISA lysis buffer supplemented with protease inhibitors, scraped into tubes, and snap-frozen in liquid nitrogen. Equal total protein amounts were added to a 96-well dish coated with the Rho binding domain of Rho effector proteins (which bind active GTP-bound Rho) in triplicate and incubated at 4 °C for 30 min with vigorous shaking. Active Rho levels were determined by subsequent incubations with anti-Rho antibody and secondary horseradish peroxidase-conjugated antibody for 60 min each with vigorous shaking at room temperature. Active Rho was determined by measuring absorbance at 490 nm using an ELISA plate reader after subtraction from a sample only containing lysis buffer. Relative Rho activity was determined by dividing the mean absorbance of si-RNA treated lysates by the mean absorbance of those obtained from control neurons. Experiments were repeated three times.

Statistical analysis

Statistical analysis was performed employing the Graphpad Prism 5.0 software. Pairwise comparison employing Student's *t*-test was performed in Figs. 2 and 5B (left panel), and Supplementary Figs. 1B and 2. One-way ANOVA with Tukey correction for multiple comparisons was used in Fig. 4A. Two-way ANOVA with Tukey and Bonferroni correction for multiple comparisons were used in Figs. 3B, 4 and 6. Data from Fig. 5B (right panel) were analyzed by X^2 to assess the significance in both distributions (number of axons, Zar, 1984). The *P*-values are indicated in the corresponding figure legend.

Acknowledgments

We are indebted to L. Mongiat for critical reading of the manuscript. We thank M. Bisbal for advice on cultures and immunohistochemistry, P. Schielman for advice on statistical analysis and to L. Binder for the Tau-1 antibody.

MFC, AFS and AC are members of the Argentine Research Council (CONICET). DLF holds a postdoctoral fellowship and CR was supported by a graduate fellowship from CONICET. This work was supported by two grants from the Agencia Nacional para la Promoción de Ciencia y Tecnología (ANPCyT, nos. 01-13823 and 678) and from the NIH-USA (1R21TW008430) to MFC and by the HHMI International Research Program (no. 55005963) to AFS.

Appendix A. Supplementary data

Supplementary data associated with this article can be found, in the online version, at doi:10.1016/j.mcn.2010.03.004.

References

Applewhite, D.A., Barzik, M., Kojima, S., Svitkina, T.M., Gertler, F.B., Borisy, G.G., 2007. Ena/VASP proteins have an anti-capping independent function in filopodia formation. Mol. Biol. Cell 18, 2579–2591.

Arimura, N., Kaibuchi, K., 2007. Neuronal polarity: from extracellular signals to intracellular mechanisms. Nat. Rev. Neurosci. 8, 194–205.

Bartlett, W.P., Banker, G.A., 1984. An electron microscopic study of the development of axons and dendrites by hippocampal neurons in culture: I. Cells which develop without intercellular contacts. J. Neurosci. 4, 1944–1953.

Bear, J.E., Svitkina, T.M., Krause, M., Schafer, D.A., Loureiro, J.J., Strasser, G.A., Maly, I.V., Chaga, O.Y., Cooper, J.A., Borisy, G.G., Gertler, F.B., 2002. Antagonism between Ena/VASP proteins and actin filament capping regulates fibroblast motility. Cell 109, 509–521.

Bito, H., Furuyashiki, T., Ishihara, H., Shibasaki, Y., Ohashi, K., Mizuno, K., Maekawa, M., Ishizaki, T., Narumiya, S., 2000. A critical role for a Rho-associated kinase, p160ROCK, in determining axon outgrowth in mammalian CNS neurons. Neuron 26, 431–441.

Bossy-Wetzel, E., Schwarzenbacher, R., Lipton, S.A., 2004. Molecular pathways to neurodegeneration. Nat. Med. 10, S2–S9 Suppl.

Bradke, F., Dotti, C.G., 2000. Differentiated neurons retain the capacity to generate axons from dendrites. Curr. Biol. 10, 1467–1470.

Bredesen, D.E., Rao, R.V., Mehlen, P., 2006. Cell death in the nervous system. Nature 443, 796–802.

Butt, E., Abel, K., Krieger, M., Palm, D., Hoppe, V., Hoppe, J., Walter, U., 1994. cAMP- and cGMP-dependent protein kinase phosphorylation sites of the focal adhesion vasodilator-stimulated phosphoprotein (VASP) in vitro and in intact human platelets. J. Biol. Chem. 269, 14509–14517.

Caceres, A., Banker, G.A., Binder, L., 1986. Immunocytochemical localization of tubulin and microtubule-associated protein 2 during the development of hippocampal neurons in culture. J. Neurosci. 6, 714–722.

Cao, X., Sudhof, T.C., 2001. A transcriptionally [correction of transcriptively] active complex of APP with Fe65 and histone acetyltransferase Tip60. Science 293, 115–120.

Comer, A.R., Ahern-Djamali, S.M., Juang, J.L., Jackson, P.D., Hoffmann, F.M., 1998. Phosphorylation of Enabled by the Drosophila Abelson tyrosine kinase regulates the in vivo function and protein–protein interactions of Enabled. Mol. Cell. Biol. 18, 152–160.

Conde, C., Caceres, A., 2009. Microtubule assembly, organization and dynamics in axons and dendrites. Nat. Rev. Neurosci. 10, 319–332.

Da Silva, J.S., Medina, M., Zuliani, C., Di Nardo, A., Witke, W., Dotti, C.G., 2003. RhoA/ROCK regulation of neuritogenesis via profilin IIa-mediated control of actin stability. J. Cell Biol. 162, 1267–1279.

Dent, E.W., Kwiatkowski, A.V., Mebane, L.M., Philippar, U., Barzik, M., Rubinson, D.A., Gupton, S., Van Veen, J.E., Furman, C., Zhang, J., Alberts, A.S., Mori, S., Gertler, F.B., 2007. Filopodia are required for cortical neurite initiation. Nat. Cell Biol. 9, 1347–1359.

Dotti, C.G., Poo, M.M., 2003. Neuronal polarization: building fences for molecular segregation. Nat. Cell Biol. 5, 591–594.

Dotti, C.G., Sullivan, C.A., Banker, G.A., 1988. The establishment of polarity by hippocampal neurons in culture. J. Neurosci. 8, 1454–1468.

Drees, F., Gertler, F.B., 2008. Ena/VASP: proteins at the tip of the nervous system. Curr. Opin. Neurobiol. 18, 53–59.

Ermekova, K.S., Zambrano, N., Linn, H., Minopoli, G., Gertler, F., Russo, T., Sudol, M., 1997. The WW domain of neural protein FE65 interacts with proline-rich motifs in Mena, the mammalian homolog of Drosophila enabled. J. Biol. Chem. 272, 32869–32877.

Gallo, G., Yee Jr., H.F., Letourneau, P.C., 2002. Actin turnover is required to prevent axon retraction driven by endogenous actomyosin contractility. J. Cell Biol. 158, 1219–1228.

Galvan, V., Gorostiza, O.F., Banwait, S., Ataie, M., Logvinova, A.V., Sitaraman, S., Carlson, E., Sagi, S.A., Chevallier, N., Jin, K., Greenberg, D.A., Bredesen, D.E., 2006. Reversal of Alzheimer's-like pathology and behavior in human APP transgenic mice by mutation of Asp664. Proc. Natl. Acad. Sci. U. S. A. 103, 7130–7135.

Gertler, F.B., Niebuhr, K., Reinhard, M., Wehland, J., Soriano, P., 1996. Mena, a relative of VASP and Drosophila Enabled, is implicated in the control of microfilament dynamics. Cell 87, 227–239.

Giesemann, T., Schwarz, G., Nawrotzki, R., Berhorster, K., Rothkegel, M., Schluter, K., Schrader, N., Schindelin, H., Mendel, R.R., Kirsch, J., Jockusch, B.M., 2003. Complex formation between the postsynaptic scaffolding protein gephyrin, profilin, and Mena: a possible link to the microfilament system. J. Neurosci. 23, 8330–8339.

Gomis-Ruth, S., Wierenga, C.J., Bradke, F., 2008. Plasticity of polarization: changing dendrites into axons in neurons integrated in neuronal circuits. Curr. Biol. 18, 992–1000.

Graham, R.K., Deng, Y., Slow, E.J., Haigh, B., Bissada, N., Lu, G., Pearson, J., Shehadeh, J., Bertram, L., Murphy, Z., Warby, S.C., Doty, C.N., Roy, S., Wellington, C.L., Leavitt, B.R., Raymond, L.A., Nicholson, D.W., Hayden, M.R., 2006. Cleavage at the caspase-6 site is required for neuronal dysfunction and degeneration due to mutant huntingtin. Cell 125, 1179–1191.

Higashi, M., Ishikawa, C., Yu, J., Toyoda, A., Kawana, H., Kurokawa, K., Matsuda, M., Kitagawa, M., Harigaya, K., 2009. Human Mena associates with Rac1 small GTPase in glioblastoma cell lines. PLoS ONE 4, e4765.

Ikin, A.F., Sabo, S.L., Lanier, L.M., Buxbaum, J.D., 2007. A macromolecular complex involving the amyloid precursor protein (APP) and the cytosolic adapter FE65 is a negative regulator of axon branching. Mol. Cell. Neurosci. 35, 57–63.

Ishizaki, T., Uehata, M., Tamechika, I., Keel, J., Nonomura, K., Maekawa, M., Narumiya, S., 2000. Pharmacological properties of Y-27632, a specific inhibitor of rho-associated kinases. Mol. Pharmacol. 57, 976–983.

Jalink, K., van Corven, E.J., Hengeveld, T., Morii, N., Narumiya, S., Moolenaar, W.H., 1994. Inhibition of lysophosphatidate- and thrombin-induced neurite retraction and neuronal cell rounding by ADP ribosylation of the small GTP-binding protein Rho. J. Cell Biol. 126, 801–810.

Kajiwara, Y., Akram, A., Katsel, P., Haroutunian, V., Schmeidler, J., Beecham, G., Haines, J.L., Pericak-Vance, M.A., Buxbaum, J.D., 2009. FE65 binds Teashirt, inhibiting expression of the primate-specific caspase-4. PLoS ONE 4, e5071.

Katoh, H., Aoki, J., Ichikawa, A., Negishi, M., 1998. p160 RhoA-binding kinase ROKalpha induces neurite retraction. J. Biol. Chem. 273, 2489–2492.

Kwiatkowski, A.V., Rubinson, D.A., Dent, E.W., Edward, v.V., Leslie, J.D., Zhang, J., Mebane, L.M., Philippar, U., Pinheiro, E.M., Burds, A.A., Bronson, R.T., Mori, S., Fassler, R., Gertler, F.B., 2007. Ena/VASP is required for neuritogenesis in the developing cortex. Neuron 56, 441–455.

Lanier, L.M., Gates, M.A., Witke, W., Menzies, A.S., Wehman, A.M., Macklis, J.D., Kwiatkowski, D., Soriano, P., Gertler, F.B., 1999. Mena is required for neurulation and commissure formation. Neuron 22, 313–325.

Lebrand, C., Dent, E.W., Strasser, G.A., Lanier, L.M., Krause, M., Svitkina, T.M., Borisy, G.G., Gertler, F.B., 2004. Critical role of Ena/VASP proteins for filopodia formation in neurons and in function downstream of netrin-1. Neuron 42, 37–49.

Lessing, D., Bonini, N.M., 2009. Maintaining the brain: insight into human neurodegeneration from Drosophila melanogaster mutants. Nat. Rev. Genet. 10, 359–370.
Li, W., Li, Y., Gao, F.B., 2005. Abelson, enabled, and p120catenin exert distinct effects on dendritic morphogenesis in Drosophila. Dev. Dyn. 234, 512–522.
Lin, Y.L., Lei, Y.T., Hong, C.J., Hsueh, Y.P., 2007. Syndecan-2 induces filopodia and dendritic spine formation via the neurofibromin-PKA-Ena/VASP pathway. J. Cell Biol. 177, 829–841.
Linseman, D.A., Laessig, T., Meintzer, M.K., McClure, M., Barth, H., Aktories, K., Heidenreich, K.A., 2001. An essential role for Rac/Cdc42 GTPases in cerebellar granule neuron survival. J. Biol. Chem. 276, 39123–39131.
Luo, L., 2002. Actin cytoskeleton regulation in neuronal morphogenesis and structural plasticity. Annu. Rev. Cell Dev. Biol. 18, 601–635.
Luo, L., O'Leary, D.D., 2005. Axon retraction and degeneration in development and disease. Annu. Rev. Neurosci. 28, 127–156.
Luo, L., Liao, Y.J., Jan, L.Y., Jan, Y.N., 1994. Distinct morphogenetic functions of similar small GTPases: Drosophila Drac1 is involved in axonal outgrowth and myoblast fusion. Genes Dev. 8, 1787–1802.
Mattson, M.P., Magnus, T., 2006. Ageing and neuronal vulnerability. Nat. Rev. Neurosci. 7, 278–294.
McMurray, C.T., 2000. Neurodegeneration: diseases of the cytoskeleton? Cell Death Differ. 7, 861–865.
Menzies, A.S., Aszodi, A., Williams, S.E., Pfeifer, A., Wehman, A.M., Goh, K.L., Mason, C.A., Fassler, R., Gertler, F.B., 2004. Mena and vasodilator-stimulated phosphoprotein are required for multiple actin-dependent processes that shape the vertebrate nervous system. J. Neurosci. 24, 8029–8038.
Myers, K.A., He, Y., Hasaka, T.P., Baas, P.W., 2006. Microtubule transport in the axon: rethinking a potential role for the actin cytoskeleton. Neuroscientist 12, 107–118.
Nakayama, A.Y., Harms, M.B., Luo, L., 2000. Small GTPases Rac and Rho in the maintenance of dendritic spines and branches in hippocampal pyramidal neurons. J. Neurosci. 20, 5329–5338.
Ona, V.O., Li, M., Vonsattel, J.P., Andrews, L.J., Khan, S.Q., Chung, W.M., Frey, A.S., Menon, A.S., Li, X.J., Stieg, P.E., Yuan, J., Penney, J.B., Young, A.B., Cha, J.H., Friedlander, R.M., 1999. Inhibition of caspase-1 slows disease progression in a mouse model of Huntington's disease. Nature 399, 263–267.
Palop, J.J., Chin, J., Mucke, L., 2006. A network dysfunction perspective on neurodegenerative diseases. Nature 443, 768–773.
Rezával, C., Berni, J., Gorostiza, E.A., Werbajh, S., Fagilde, M.M., Fernandez, M.P., Beckwith, E.J., Aranovich, E.J., Garcia, C.A., Ceriani, M.F., 2008. A functional misexpression screen uncovers a role for enabled in progressive neurodegeneration. PLoS ONE 3, e3332.
Sabo, S.L., Ikin, A.F., Buxbaum, J.D., Greengard, P., 2001. The Alzheimer amyloid precursor protein (APP) and FE65, an APP-binding protein, regulate cell movement. J. Cell Biol. 153, 1403–1414.
Sanchez, M., Gastaldi, L., Remedi, M., Caceres, A., Landa, C., 2008. Rotenone-induced toxicity is mediated by Rho-GTPases in hippocampal neurons. Toxicol. Sci. 104, 352–361.
Sanchez-Soriano, N., Tear, G., Whitington, P., Prokop, A., 2007. Drosophila as a genetic and cellular model for studies on axonal growth. Neural Dev. 2, 9.
Trulzsch, B., Garnett, C., Davies, K., Wood, M., 2007. Knockdown of SMN by RNA interference induces apoptosis in differentiated P19 neural stem cells. Brain Res. 1183, 1–9.
Zambrano, N., Minopoli, G., De Candia, P., Russo, T., 1998. The Fe65 adaptor protein interacts through its PID1 domain with the transcription factor CP2/LSF/LBP1. J. Biol. Chem. 273, 20128–20133.
Zar, J.H., 1984. Biostatistical Analysis. Prentice Hall, New Jersey.